THE JOURNAL OF PHYSICAL CHEMISTRY B

Article

pubs.acs.org/JPCB

The Polysiloxane Cyclization Equilibrium Constant: A Theoretical Focus on Small and Intermediate Size Rings

Claire Madeleine-Perdrillat,[†] Florence Delor-Jestin,[†,‡] and Pascal de Sainte Claire*[,†,‡]

[†]CNRS, UMR 6296, Institut de Chimie de Clermont Ferrand (ICCF), Photochimie, BP 80026, F-63171 Aubière, France

[‡]Clermont Université, ENSCCF, BP 10448, F-63000, Clermont Ferrand, France

Supporting Information

ABSTRACT: The nonlinear dependence of polysiloxane cyclization constants ($\log(K_x)$) with ring size ($\log(x)$) is explained by a thermodynamic model that treats specific torsional modes of the macromolecular chains with a classical coupled hindered rotor model. Several parameters such as the dependence of the internal rotation kinetic energy matrix with geometry, the effect of potential energy hindrance, anharmonicity, and the couplings between internal rotors were investigated. This behavior arises from the competing effects of local molecular entropy that is mainly driven by the intrinsic transformation of vibrations in small cycles into hindered rotations in larger cycles and configurational entropy.

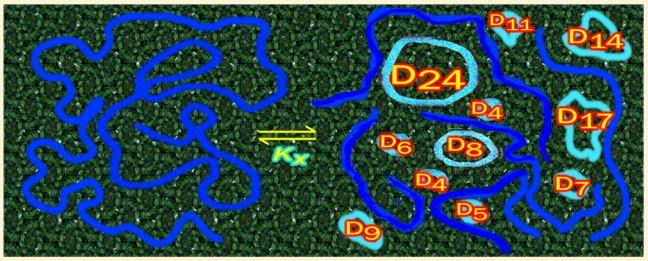

1. INTRODUCTION

The intramolecular cyclization mechanism of macromolecules has been the subject of experimental and theoretical attention for a long time.[1,2] It can be described by the equilibrium between an n-mer L_n macromolecule and D_x cycles, where x is the number of monomer units in D_x: $L_n \leftrightharpoons L_{n-x} + D_x$. The equilibrium constant K_x^n is independent of n for long chains ($\lim_{n\to\infty} K_x^n = K_x$). Thus, in that case, the distribution of x depends only on experimental conditions.

Experimental studies focused on the dependence of ring size distributions and equilibrium constants on temperature, molecular weights, and dilution conditions. On the other hand, the theory of intramolecular cyclization reactions, based on the rotational isomeric state (RIS) model, was able to reproduce with great accuracy the equilibrium constant and distribution of the equilibrated ring fraction.[3−6]

Among the large variety of macromolecules that undergo intramolecular cyclization reactions, the polysiloxane family has received particular attention because significant amounts of cyclic molecules are invariably obtained at equilibrium.[2,7−9] This property is an important issue in studies of thermo- or photodegradation mechanisms of polysiloxanes.[10−18] For example, the weight fraction of cyclic siloxanes in undiluted polydimethylsiloxanes (PDMS) is 18.3% at T = 383 K.[7] This is due to the important backbone flexibility of siloxane polymers. In addition, polymer dilution favors intramolecular cyclization reactions and the ring weight fraction increases with dilution. Last, for small cycles, the chain-ring equilibrium constant increases with substituent size, while the opposite is observed for the larger rings.[2,7]

The precursor work of Flory[4−6] was able to explain the linear relationship between K_x and $x^{-5/2}$ for polysiloxanes with the RIS model by showing the key role of the statistical distribution of mer-unit configurations. However, their model failed to reproduce the oscillating behavior of K_x for small cycles, i.e., $x < 20$ (see Figure 1). It is the goal of this work to explain the complex dependence of K_x for small values of x. Our study is

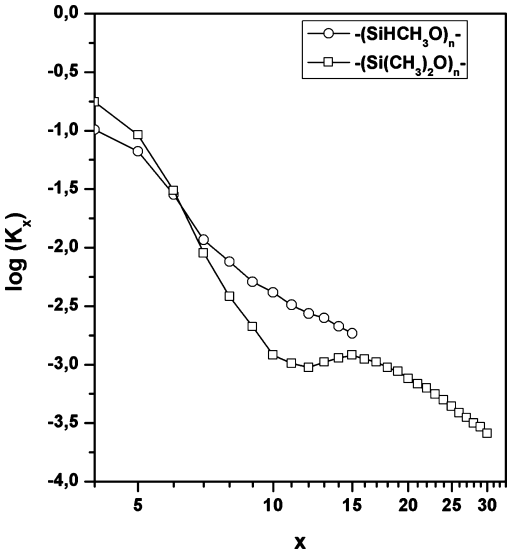

Figure 1. Experimental molar cyclization equilibrium constants (mol/L) in undiluted equilibrates of polyhydrogenmethylsiloxanes (○, T = 273 K) and polydimethylsiloxanes (□, T = 383 K). x represents the number of $-(SiH_2O)-$ or $-(SiMe_2O)-$ units in D_x cycles. For large values of x, $K_x \sim x^{-5/2}$. Experimental data from ref 7.

Received: September 3, 2013
Revised: December 10, 2013
Published: December 10, 2013

 © 2013 American Chemical Society

based on ab initio calculations and an accurate thermodynamic description of the cyclization constant. In our work, the numerous internal rotors in polysiloxane macromolecules are treated classically with a coupled hindered rotor model.

2. GENERAL COMPUTATIONAL PROCEDURE

In this work, L_n is a hydroxy terminated polydihydrogensiloxane HO−$(SiH_2O)_n$−H. Thus, the smallest linear fragment L_0 is H_2O. In that case, the respective cycle is D_n. The calculation of the cyclization constant is performed here for the arbitrary large value n = 1000. Results are independent of n, provided it is large enough. Our strategy aims at computing the thermodynamic values of small linear chains and extrapolating these quantities for large values of n.

The hydrogen terminated disiloxane molecule ($H_3SiOSiH_3$) was used to determine the best theoretical calculation method that gives good geometrical parameters and bond dissociation enthalpies.

Geometries and Electronic Energy. In comparison to carbon-based polymers, polysiloxanes are highly flexible molecules.[18−20] The small linearization energy of the Si−O−Si angle and the smaller than usual Si−O bond length (∼1.64 Å) arise mostly from the partial ionic character of the Si−O bond.[21,22] The theoretical Si−O bond dissociation enthalpy of disiloxane was previously calculated: it is 131.0 kcal/mol at 298 K at the G2 level,[23] and the experimental Si−O bond length and Si−O−Si angle in disiloxane are 1.634 Å and 144.1°, respectively.[24] Isodesmic reactions of alkyl siloxanes were also studied in order to model extended siloxane systems from single building blocks.[25] The B3LYP/6-311+G(d,p) method was selected on the basis of a small variation of the reaction energy. However, the Si−O bond dissociation energy and Si−O−Si bond angle are poor at this level of theory (respectively 115.9 kcal/mol[26] and 180° for the disiloxane molecule[25]). In another study, it was shown that accurate geometries were obtained if 2d polarization functions were included in the basis set.[27] In addition, good linearization energies were obtained with the MP2 method. In light of these results, it was decided in our work to optimize the geometries and perform vibrational analyses at the HF/6-31G(2d) level. Energies were computed at the MP2/6-31G(2d)//HF/6-31G(2d) level of theory, a method that enabled calculations of large molecules. The calculated Si−O−Si bond angle, Si−O bond length, and Si−O bond dissociation enthalpy at 298 K for disiloxane are, respectively, 142.7°, 1.633 Å, and 128.5 kcal/mol[28] at this level, in good agreement with the experimental results, i.e., 144.1° and 1.634 Å,[22] and the theoretical G2 enthalpy of 131.0 kcal/mol.[23] Last, it should be noted that, while the DFT method B3LYP/6-311++G(2df,2p) reproduced accurately the vibrational spectrum of disiloxane,[29] the Si−O bond dissociation enthalpy was too small (118.6 kcal/mol at 298 K) at this level.[26]

Partition Functions. The cyclization equilibrium constant $K_x = \exp(-\Delta G/RT)$ was obtained from the partition functions of the linear and cyclic species. The separability of the translational, overall rotational, vibrational, and electronic degrees of freedom was assumed. In our work, the electronic partition functions were set to unity and the translational and overall rotational contributions were treated within the classical mechanics framework. The vibrational part was treated differently: in the highly flexible polysiloxane molecules, a number of degrees of freedom are poorly described by vibrational partition functions and should be accounted for by hindered rotor partition functions. For example, there are $2n$ internal rotor modes in the hydroxy terminated polydihydrogensiloxane L_n (HO−$(SiH_2O)_n$−H), i.e., $2n$ internal rotations about the Si−O bonds. The global partition function for L_n may be written:

$$q(L_n) = q_{\text{trans}} \times q_{\text{rot}} \times \prod_{i=1}^{10n+3} q_{\text{vib}}^{i} \times \prod_{j=1}^{2n} q_{\text{hr}}^{j} \quad (1)$$

In this equation, *hr* stands for hindered rotor. The couplings between vibrations and internal rotations are neglected, and q_{hr} is obtained by an exact classical treatment of the coupled hindered rotors (see below). The anharmonicity contribution to q_{vib}^{i} was computed for the pure vibrational modes with the perturbation theory method proposed by Truhlar et al. for the linear and cyclic hydrogensiloxanes.[30−33]

The internal rotor modes were first identified visually, and the respective harmonic vibrational frequencies were removed from the set of pure vibrational modes. All the degrees of freedom of the small cycles (x = 2−5) were treated as pure vibrations. In addition, when cycles become large, our model accounts for the change of intrinsic character of the Si−O torsional modes from pure vibration to internal rotation because the cycle tension disappears in large cycles.

The classical partition function q_{hr} for a set of $2n$ rotors is[34]

$$q_{\text{hr}} = \left(\frac{2\pi k_B T}{h^2}\right)^n \int_0^{2\pi} \cdots \int_0^{2\pi} [D(\varphi_1, ..., \varphi_{2n})]^{1/2} e^{-V(\varphi_1,...,\varphi_{2n})/k_B T} \, d\varphi_1 \ldots d\varphi_{2n} \quad (2)$$

where $[D]$ is the determinant of the kinetic energy matrix of the coupled internal rotors. The symmetry numbers of the respective internal rotors were set to unity. In this equation, $[D]$ is computed according to the procedure described in ref 35 for Pitzer rotors.[36] The kinetic energy matrix of the system of the $2n$ coupled internal rotors is written in a fixed reference frame and then decoupled from overall rotation and translation. This procedure yields the $(2n)^2$ kinetic energy matrix for internal rotation. Its diagonal elements are the reduced moments of inertia for each internal rotor, while the off-diagonal terms represent the coupling between internal rotors. This procedure is similar to that reported in refs 37 and 38.[39]

In eq 2, $V(\varphi_1, ..., \varphi_{2n})$ is the multidimensional potential energy surface (PES) for internal rotation. The calculation of $V(\varphi_1, ..., \varphi_{2n})$ remains a formidable task, and it was necessary to make approximations at this point. In our work, the PES was decoupled into $2n$ monodimensional potential energy terms $V(\varphi_i)$, i.e., $V(\varphi_1, ..., \varphi_{2n}) = \sum_{i=1}^{2n} V(\varphi_i)$. However, it was shown that including two-dimensional PES contributions and kinetic couplings improved the partition function of linear *n*-alkanes.[37,38] The high flexibility of polysiloxane molecules renders this approach extremely difficult because there are a number of low-lying structures close to the global minimum. Thus, for polysiloxanes, the monodimensional potential terms $V(\varphi_i)$ are strongly coupled. However, the barriers for internal rotation are much smaller than those in *n*-alkanes, and the magnitude of this coupling is smaller as well. To circumvent this problem, the potential energy terms $V(\varphi_i)$ were computed by scanning φ_i and freezing all the other $2n - 1$ Si−O dihedral angles along the molecular backbone at their respective value in the equilibrium geometry. The remaining degrees of freedom were allowed to relax.

dx.doi.org/10.1021/jp4088157 | J. Phys. Chem. B 2014, 118, 330−336

Table 1. MP2/6-31G(2d)//HF/6-31G(2d) Electronic Energy, Enthalpy, and Entropy Contributions to the Overall Free Energy of Cyclic (D_x = $(SiH_2O)_x$; $2 \le x \le 5$) and Linear (L_n = HO−$(SiH_2O)_n$−H; n = 3−4) Polydihydrogensiloxanes[a]

	sym[b]	E^c (mer-unit)	H_{ho}	H_{anh}	S_{ho}	S_{anh}
D_2	D_{2h}	−365.30659258	32.5	32.3	67.4	67.5
D_3	D_{3h}	−365.33046146	49.9	49.5	84.2	84.3
D_4	S_4	−365.33287679	66.9	66.5	103.3	103.2
D_5		−365.33339829	83.9	83.4	122.6	121.6

	E^c (mer-unit)	H_{ho}	H_{ho}^{chr} [d]	H_{anh}^{chr}	S_{ho}	S_{ho}^{chr}	S_{anh}^{chr}	S_{anh}^{-chr}
L_3	−365.33175247	67.3	67.5	67.0	111.6	117.0	117.5	119.2
L_4	−365.33211955	84.3	84.1	83.6	134.2	142.0	142.8	146.1

[a]Labels: ho = harmonic oscillator approximation for all modes (no hindered rotors), anh = anharmonicity included for the vibrational modes, chr = hindered rotors are coupled, −chr = hindered rotors are not coupled. T = 273.15 K. Units: E in au, H in kcal/mol (includes RT), S in cal/mol/K. [b]Point group symmetry. [c]Electronic energy per SiH_2O unit. For L_3 and L_4, this energy is $(E(L_n) - E(H_2O))/n$. $E(H_2O)$ = −76.22532522 au. [d]The hindered rotor coupling terms cancel out in the expression of H, and $H_{anh}^{chr} = H_{anh}^{-chr}$.

The dependence of D on internal rotation angles φ_i was also examined, i.e., the multidimensional coupling of the kinetic energy matrix with geometry. Note that this is different from the coupling of internal rotors at a specific geometry, an effect which is fully accounted for by our computing treatment (see above). It was decided to follow a procedure that was similar to that used for the potential terms: $[D(\varphi_1, ..., \varphi_{2n})]$ was computed at the equilibrium geometry, i.e., $[D_0\ (\varphi_1^0, ..., \varphi_{2n}^0)]$, and decoupled into one-dimensional terms that accounted for the variation of D_0 with respect to internal rotation angles through a correlation function $f(\varphi_i)$:[37,38]

$$[D(\varphi_1, ..., \varphi_{2n})] = [D_0(\varphi_1^0, ..., \varphi_{2n}^0)] \times \prod_{i=1}^{2n} f(\varphi_i) \tag{3}$$

In this equation, $[D_0\ (\varphi_1^0, ..., \varphi_{2n}^0)] \times f(\varphi_i)$ represents the variation of $[D(\varphi_1, ..., \varphi_{2n})]$ in the one-dimensional potential energy $V(\varphi_i)$.[40] It will be shown in the Results section that the effect of the correlation function is negligible in our case. q_{hr} was thus computed as follows:

$$q_{hr} = \left(\frac{2\pi k_B T}{h^2}\right)^n [D_0(\varphi_1^0, ..., \varphi_{2n}^0)]^{1/2} \prod_{i=1}^{2n} \int_0^{2\pi} f(\varphi_i) \times e^{-V(\varphi_i)/k_B T}\, d\varphi_i \tag{4}$$

Finally, the equilibrium constant is

$$K_x = \frac{\propto}{2x} e^{\Delta S/R} \times e^{-\Delta E_{el}/RT} \times e^{-\Delta H/RT} \tag{5}$$

The symmetry numbers of the linear species[1,4−6,41] L_n and L_{n-x} cancel in the final expression of K_x, contrarily to the symmetry number of D_x: in cyclic polydihydrogensiloxanes, the barrier that separates conformations with equivalent hydrogen atoms is small, hence the symmetry number of $2x$ in eq 5 for all of the cycles. This procedure was previously used in theoretical treatments of cycloalkanes[41] and polydimethylsiloxanes.[4]

In eq 5, ΔS, ΔE_{el}, and ΔH represent the variations of cyclization entropy, electronic energy, and thermal contribution to enthalpy, respectively. In addition, in our work, free energies obtained from quantum calculations used a reference state of 1 atm.[42] It was thus necessary to correct our results for a reference state of 1 mol/L, i.e., $\alpha = 1/0.82057T$ in eq 5.[43]

3. CALCULATION OF THERMODYNAMIC PROPERTIES

The goal of the theoretical calculations was first to compute the thermodynamic quantities per −(SiH_2O)− unit in eq 5 for small and intermediate molecular sizes, in order to be able to extrapolate these values for larger cycles and linear chains.

Small Size Model Molecules. The optimizations and normal-mode analyses of cyclic (D_x) and linear (L_n) polydihydrogensiloxane molecules were performed at the HF/6-31G(2d) level, whereas electronic energies were computed with the MP2/6-31G(2d)//HF/6-31G(2d) method. The effect of anharmonicity was investigated for the pure vibrational part of the partition function, and the importance of hindered rotor couplings was studied. The respective enthalpy and entropy contributions to the overall free energy are given in Table 1 for all of these species for a temperature of 273.15 K. First, the anharmonic contribution appears to be small for L_4 (less than 1%), while including the hindered rotor treatment in the model amounts up to a 6% difference with the pure harmonic oscillator model for the entropic part of the free energy. Note that the coupling of the hindered rotors reduces this discrepancy by roughly 3%. In addition, this effect increases with n. Thus, considering the cyclization equilibrium $L_n \leftrightharpoons L_{n-x} + D_x$ and the cancellation of $2(n - x)$ hindered rotor partition functions in the equilibrium constant, one is left with the contribution of $2x$ hindered rotors in the final result. This discrepancy may become extremely important for medium to large cycle sizes ($n > 5$). This is shown below.

Extrapolation Model from Small to Large Size Species. The electronic energy per mer-unit was fit to an exponential decay function $E(x) = E_0 + c_1 \times \exp(-x/c_2)$ for the cycles. E_0 = −365.33332 au was found for polydihydrogensiloxanes (the convergence of $E(x)$ for the cycles and chains is provided in Figure S1 in the Supporting Informations). This value was used in turn for the energy per mer-unit for the chains. E_0 was obtained from extrapolation of the energy of the cyclic species exclusively, in order to prevent contributions of the local interactions that appeared in the optimization of linear chains because of folded structures. Thus, $E(L_n) = E(L_4) + (n - 4) \times E_0$ and $E(D_x) = x \times E_0$ were used to compute the electronic energies of the chains and the cycles, respectively. The calculation of the enthalpy and entropy contributions for L_n is detailed now.

The translational and rotational parts of the enthalpy amounts to $3RT$ for L_n. The translational entropy is $S_{trans}(L_n) = S_{trans}(L_4) + 1.5R \times \ln[(M_{H_2O} + nM_{mer})/(M_{H_2O} + 4M_{mer})]$, where M_{H_2O} and M_{mer} are the molar masses of H_2O and SiH_2O. The contributions from the vibrational and hindered rotor degrees of freedom were calculated for L_n with $H_{vib/hr}(L_n) = H_{vib/hr}(L_4) + (n - 4) \times [H_{vib/hr}(L_4) - H_{vib/hr}(L_3)]$. Thus, $H(L_n)$

dx.doi.org/10.1021/jp4088157 | J. Phys. Chem. B 2014, 118, 330−336

$= 4RT + H_{vib/hr}(L_n)$.[44] The vibrational/hindered rotor entropy contribution was computed similarly.

The rotational part of the entropy for the cycles ($2 \le x \le 5$) and the chains ($1 \le n \le 4$) was fit simultaneously for the cycles and chains with $S_{rot}(x) = c_3 + c_4 \times \ln(x - c_5)$ and $S_{rot}(n) = c_3 + c_4 \times \ln(n + c_6 - c_5)$, respectively. c_6 is a parameter that accounts for the chain ends in L_n (H and OH). The definition of mer-unit is not the same in cycles and short chains because the contributions of the chain ends amount to that of a fraction of a mer-unit. This fraction is accounted for by c_6. In these expressions, c_3 = 22.78 cal/mol/K, c_4 = 6.052 cal/mol/K, c_5 = 0.659, and c_6 = 0.7. The latter value (c_6 = 0.7) shows that the contributions of the chain ends to the rotational part of the entropy amount to 70% of that of a cycle mer-unit. The fit is shown in Figure S2 in the Supporting Informations. It was important to use here the same function for both chains and cycles in order to prevent unphysical divergence of K_x at large x values.

The calculation of H and S for D_x bears more complexity. This is discussed now.

The translational and rotational parts of the enthalpy are also $3RT$ for D_x. The translational entropy is $S_{trans}(D_x) = S_{trans}(D_5) + 1.5R \times \ln[x/5]$. This equation holds for $x \ge 5$. The rotational contribution to the entropy is described above (see also Figure S2 in the Supporting Informations). The contribution of the vibrational degrees of freedom was calculated for the small cycles (see Table 1). However, among these modes, there are $2x$ degrees of freedom that undergo a change of intrinsic character from pure vibrations for small x to hindered internal rotations for large cycles. The hindered rotor contribution per mer-unit for large cycles should not be different from that of the large chains. Thus, switching functions $W_H(D_x)$ and $W_S(D_x)$ that accounted for this change were included in our model. These functions switched between the thermodynamic value (H or S) per mer-unit calculated for D_5 and the respective asymptotic value of a large chain taken as the difference between that of L_5 and L_4:

$$W_H(D_x) = H^{L_4}_{vib/hr} - H^{L_3}_{vib/hr} + \frac{H^{D_5}_{vib/hr}/5 - (H^{L_4}_{vib/hr} - H^{L_3}_{vib/hr})}{1 + \left(\frac{x-5}{p_1}\right)^{p_2}} \quad (6)$$

$W_S(D_x)$ is calculated similarly. In this equation, p_1 and p_2 are parameters that control the position and suddenness of the switch. For example, for p_1 = 8, the $2x$ degrees of freedom bear mixed 50/50 pure vibrational/hindered rotor character at $x = 5 + p_1$, i.e., x = 13. Small values for p_2 contribute to smoothing the switch over a large range of x (see Figure S3 in the Supporting Informations). Thus, these parameters give physical insights of the cyclization mechanism. The vibrational/hindered rotor parts were computed for the cycles with $H_{vib/hr}(D_x) = x \times W_H(D_x)$ and $S_{vib/hr}(D_x) = x \times W_S(D_x)$. The same parameters p_1 and p_2 are used throughout.

The Cyclization Constant. K_x is computed according to eq 5. However, at this point, the entropy does not converge to the RIS model for large x (see eq 7):

$$\Delta S_{trans+rot+vib/hr} = S_{trans}(D_5) + 1.5R \times \ln\left[\frac{M_{H_2O} + (n-x)M_{mer}}{M_{H_2O} + nM_{mer}} \times \frac{x}{5}\right] + \ldots c_3 + c_4 \times \ln\left[\frac{(n - x + c_6 - c_5) \times (x - c_5)}{n + c_6 - c_5}\right] + \frac{x}{1 + \left(\frac{x-5}{p_1}\right)^{p_2}} \times [S^{D_5}_{vib}/5 - (S^{L_4}_{vib/hr} - S^{L_3}_{vib/hr})] \quad (7)$$

The last term in eq 7 goes to zero for large values of x and $n \to \infty$, if $p_2 > 1$. If $p_2 = 1$ (like in our work), this term behaves like $p_1 \times [S^{D_5}_{vib}/5 - (S^{L_4}_{vib/h} - S^{L_3}_{vib/h})]$ for large x.[45] Thus, $\log(K_x)$ is proportional to $3.5 \times \log(x)$ for large cycles, i.e., $(1.5 + c_4/R - 1) \times \log(x)$ (translational, overall rotational, and cycle symmetry contributions, respectively). This is not in agreement with the RIS results of Flory et al. ($\log(K_x)$ is proportional to $-2.5 \times \log(x)$ in that case).[4−6] This is because, for large cycles, the configurational entropy contribution is predominant,[1] and transfer from translational/rotational entropy to configurational entropy occurs for intermediate cycle sizes. The origin of this effect is the decrease in the number of accessible conformations when an open chain cyclizes.[1] This change was considered in our work by including a switching function $W_{RIS}(D_x)$ that allowed smooth variation between the free energy calculated here for small to medium size rings to that obtained from the RIS model. This function is similar to that shown in eq 6 with parameters p_3 and p_4. The latter set of parameters need not be the same as p_1 and p_2 because the change of character from pure vibration into hindered rotation in cycles may not be linearly correlated with the change of accessible configurations during the cyclization. Thus, these two sets of parameters provide key details of the nature of the cyclization reaction for a specific cycle size range.

4. RESULTS

PDHS at 273.15 K. The cyclization equilibrium constant K_x was computed for polydihydrogensiloxanes (PDHS) at 273.15 K. We are not aware of experimental cyclization constants for PDHS, and it was decided to compare our results with those for polyhydrogenmethylsiloxane (PHMS). The experimental data in ref 6 show that the concavity observed within the x = 7−15 range is less pronounced when the polysiloxane bears light substituents. Since this feature is not observed for PHMS, this effect is also expected for PDHS.

Best agreement with the experimental data was reached for (p_1; p_2) = (8; 1) and (p_3; p_4) = (3; 3) (see Figure 2). In this figure, all the degrees of freedom in D_2−D_5 were treated as anharmonic vibrations. The magnitude of p_1 indicates that the respective partition functions bear 50% hindered rotor character for a cycle size of 13 mer-units (i.e., $5 + p_1$). The small value for p_2 shows that this change is soft. Also, p_3 is smaller than p_1. Thus, the configurational entropy has reached half its maximum value at D_8.[46] In the inset, $\log(K_x)$ is calculated without the contribution of the configurational entropy switching function $W_{RIS}(D_x)$. When $W_{RIS}(D_x)$ is not included in the model and for large values of x, $\log(K_x)$ is proportional to $3.5 \times \log(x)$. This linear dependence is seen in the inset for $100 < x < 10000$. This is not the correct behavior for large cycles where configurational entropy becomes predominant. This effect is taken into account by $W_{RIS}(D_x)$

dx.doi.org/10.1021/jp4088157 | J. Phys. Chem. B 2014, 118, 330−336

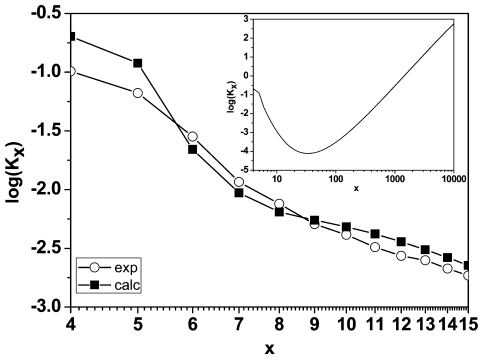

Figure 2. Calculated and experimental cyclization equilibrium constant for polydihydrogensiloxane (■, calc) and polyhydrogenmethylsiloxane (○, exp) at T = 273.15 K. (p_1; p_2) = (8; 1) and (p_3; p_4) = (3; 3) in this figure. In the inset, log(K_x) is calculated without $W_{RIS}(D_x)$. The initial macromolecular species contained 100 000 −SiH_2O− units in the inset in order to see the long-range behavior of log(K_x).

in our model. It is interesting at this point to note that these results (inset in Figure 2) show that the concavity at intermediate cycle size range is due to the change of nature of specific degrees of freedom in cyclic polysiloxanes: for small cycles, the Si−O bonds bear pure vibrational character, while, for the larger rings, such degrees of freedom are best described by hindered rotations. Including $W_{RIS}(D_x)$ in the model allows log(K_x) to catch up with the RIS model, as shown in Figure 2.

PDHS: Anharmonicity, Hindered Rotor Coupling, Temperature Effects. Several effects are investigated in this section. Results are shown in Figure 3. First, the cyclization

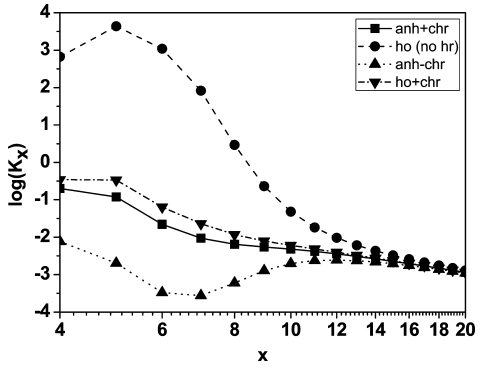

Figure 3. Calculated cyclization constant fo PDHS at T = 273.15 K. ■, full model (anharmonicity is included, and hindered rotors are coupled); ●, harmonic oscillator for all the degrees of freedom (no treatment for hindered rotors); ▲, anharmonicity for vibrational modes + hindered rotor treatment, but rotors are not coupled; ▼, harmonic oscillator for vibrational modes + coupled hindered rotor treatment. (p_1; p_2) = (8; 1) and (p_3; p_4) = (3; 3) in this figure.

constant is too large by 3−4 orders of magnitude for D_4 and D_5 when all the degrees of freedom are treated as pure vibrations within the harmonic oscillator framework (● in Figure 3). This is expected for highly flexible molecules like polysiloxanes. Second, the calculation performed with (i) the harmonic oscillator treatment of vibrational degrees of freedom and (ii) the coupled hindered rotor model for the other modes (▼ in Figure 3) gives excellent results and shows that the effect of anharmonicity is not significant (compare ▼ and ■). Last, this figure shows that the treatment of the couplings between hindered rotors is important: when this effect is not accounted for by the model, the cyclization constant is too small by more than 1 order of magnitude for small cycles (x < 8).

The dependence of K_x on temperature was also investigated by performing frequency analyses and calculation of the cyclization constant at T = 383.15 K.[47] However, the results were very similar to those computed at T = 273.15 K and they are not shown.[48]

PDHS: Effects of the Correlation Function and the Internal Rotation Potential Energy. The effect of the correlation function $f(\varphi_i)$ that accounted for the variations of the internal rotation kinetic energy matrix with torsional angles (see eq 3 and Figure S4 in the Supporting Informations) was investigated by setting $f(\varphi_i)$ = 1 for all the potential energy terms. It was found that including the correlation functions in the model had negligible effects on the calculation of the cyclization constant (see Figure 4). However, when internal

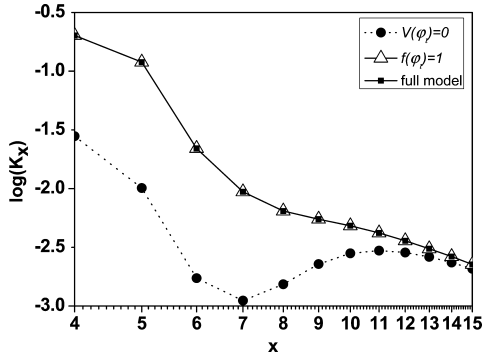

Figure 4. Calculated cyclization constant for PDHS at T = 273.15 K. ■, full model (anharmonicity is included, and hindered rotors are coupled); ●, $V(\varphi_i)$ = 0 (full model, but internal rotations are treated as free rotors); △, $f(\varphi_i)$ = 1 (full model, but the correlation functions are set to unity). (p_1; p_2) = (8; 1) and (p_3; p_4) = (3; 3) in this figure.

rotors are freely rotating ($V(\varphi_i)$ = 0), the cyclization constant is 10 times smaller than that obtained with the full coupled hindered rotor (see Figure 4). In conclusion, our model shows that both the treatment of hindered rotors and their couplings are important in order to reproduce the experimental data.

A Model for PDMS. In this section, we intend to see whether the pronounced incurvation which is observed experimentally for PDMS at x = 12 (see Figure 1) may be reproduced by our model and if physical insight may be gained from this calculation. It was decided to keep the set of parameters (p_1; p_2) identical to their previous values, i.e., (p_1; p_2) = (8; 1). In doing so, it is assumed that the change of the partition function between pure vibration and hindered rotation is similar for PDHS and PDMS.

As seen in Figure 5, good agreement is reached between experimental data and our model when (p_3; p_4) = (8, 8). In that case, p_3 > p_1 and the effect of configurational entropy starts to gain importance for larger cycle sizes (D_{13} in this case, i.e., x = 5 + p_1). This is because the repulsive interactions between the bulky substituents in PDMS reduce the number of available configurations for a given cycle size. In addition, the curvature of the concavity is governed by p_4. Thus, small curvatures are obtained for small p_4 values (smooth change). In Figure 5, p_4 is large, suggesting that the contribution of configurational entropy is rapidly predominant for x = 12 and above. This change was softer for PDHS (p_4 = 1).

dx.doi.org/10.1021/jp4088157 | J. Phys. Chem. B 2014, 118, 330−336

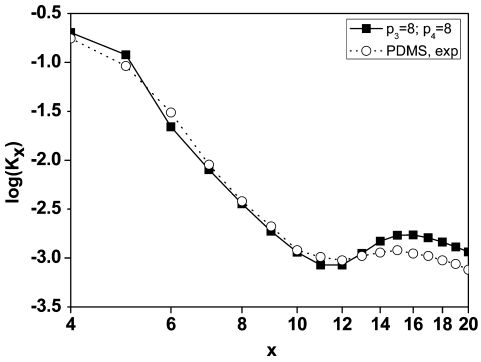

Figure 5. Experimental (○) cyclization constant for PDMS at T = 383.15 K and calculated (■) cyclization constant for PDHS at T = 273.15 K. (p_1; p_2) = (8; 1) and (p_3; p_4) = (8; 8). Anharmonicity and hindered rotor couplings are included here.

Note however that these two effects (the position of the concavity and the $W_{RIS}(D_x)$ spread) are coupled because there is a nonlinear dependence between the number of accessible configurations and x. Thus, the number of accessible configurations increases more significantly between D_{12} and D_{13}, for example, than between D_8 and D_9, and a sharper rise (large p_4) is expected for large p_3 values.

5. CONCLUSION

The cyclization of polysiloxanes is mainly governed by configurational entropy for large cycles. However, the non-monotonous behavior of the cyclization constant for intermediate and small cycle sizes remained unexplained. The cyclization reaction was investigated at the molecular level for small cycles and chains. Our model included anharmonicity and a coupled hindered rotor treatment for specific degrees of freedom. Thermodynamic quantities were extrapolated for larger species. Two constraints were included in our model: (i) the Si−O internal rotation partition functions changed from pure vibrations for small cycles to hindered rotations for large species, and (ii) the cyclization equilibrium is dominated by configurational entropy for large cycles.

Our results show that anharmonicity effects are not significant for polysiloxanes. However, it is necessary to treat the Si−O torsional modes with the hindered rotor model in order to get accurate results. Moreover, the cyclization constant is reduced by as much as 2 orders of magnitude when the couplings between hindered rotors are included. Finally, it was shown that the origin of the concavity observed experimentally for substituted polysiloxanes originates from the competition between molecular (K_x decrease) and configurational entropy (increase). For polysiloxanes that bear bulky repulsive substituents, the number of accessible configurations is reduced and configurational entropy dominates for large cycles (D_{12} for PDMS). The rapid entropy change gives rise to the incurvation in Figure 1. For PDHS, the configurational entropy is rapidly dominant, and this feature is not observed.

■ ASSOCIATED CONTENT

Ⓢ Supporting Information

The fitting functions used in this work and the general behavior of the switching function $W(D_x)$ are given in Figures S1−S4. This material is available free of charge via the Internet at http://pubs.acs.org.

■ AUTHOR INFORMATION

Corresponding Author

*E-mail: pascal.de_sainte-claire@ensccf.fr.

Notes

The authors declare no competing financial interest.

■ REFERENCES

(1) Winnik, M. A. Cyclization and the Conformation of Hydrocarbon Chains. *Chem. Rev.* **1981**, *81*, 491−524.
(2) Bischoff, R.; Cray, S. E. Polysiloxanes in Macromolecular Architecture. *Prog. Polym. Sci.* **1999**, *24*, 185−219.
(3) Jacobson, H.; Stockmayer, W. H. Intramolecular Reaction in Polycondensations. I. The Theory of Linear Systems. *J. Chem. Phys.* **1950**, *18*, 1600−1606.
(4) Flory, P. J.; Semlyen, J. A. Macrocyclization Equilibrium Constants and the Statistical Configuration of Poly(dimethylsiloxane) Chains. *J. Am. Chem. Soc.* **1966**, *88*, 3209−3212.
(5) Flory, P. J.; Suter, U. W.; Mutter, M. Macrocyclization Equilibria. 1. Theory. *J. Am. Chem. Soc.* **1976**, *98*, 5733−5739.
(6) Suter, U. W.; Mutter, M.; Flory, P. J. Macrocyclization Equilibria. 2. Poly(dimethylsiloxane). *J. Am. Chem. Soc.* **1976**, *98*, 5740−5745.
(7) Wright, P. V.; Semlyen, J. A. Equilibrium Ring Concentrations and the Statistical Conformations of Polymer Chains: Part 3. Substituent Effects in Polysiloxane Systems. *Polymer* **1970**, *11*, 462−471.
(8) Brown, J. F.; Slusarczuk, G. M. J. Macrocyclic Polydimethylsiloxanes. *J. Am. Chem. Soc.* **1965**, *87*, 931−932.
(9) Richards, R. D. C.; Hollingshurst, J.; Semlyen, J. A. Cyclic Polysiloxanes: 5. Preparation and Characterization of Poly(hydrogenmethylsiloxane). *Polymer* **1993**, *34*, 4965−4968.
(10) Grassie, N.; MacFarlane, I. G. The Thermal Degradation of Polysiloxanes − I Poly(dimethylsiloxane). *Eur. Polym. J.* **1978**, *14*, 875−884.
(11) Radhakrishnan, T. S. New Method for Evaluation of Kinetic Parameters and Mechanism of Degradation from Pyrolysis − GC Studies: Thermal Degradation of Polydimethylsiloxanes. *J. Appl. Polym. Sci.* **1999**, *73*, 441−450.
(12) Lewicki, J. P.; Liggat, J. J.; Pethrick, R. A.; Patel, M.; Rhoney, I. Investigating the Ageing Behavior of Polysiloxane Nanocomposites by Degradative Thermal Analysis. *Polym. Degrad. Stab.* **2008**, *93*, 158−168.
(13) Tanny, G. B.; St. Pierre, L. E. The Radiation Chemistry of Octamethyltrisiloxane. *J. Phys. Chem.* **1971**, *75*, 2430−2435.
(14) Radhakrishnan, T. S. Thermal Degradation of Poly(dimethylsilylene) and Poly(tetramethyldisilylene-*co*-styrene). *J. Appl. Polym. Sci.* **2006**, *99*, 2679−2686.
(15) Camino, G.; Lomakin, S. M.; Lazzari, M. Polydimethylsiloxane Thermal Degradation Part 1. Kinetic Aspects. *Polymer* **2001**, *42*, 2395−2402.
(16) Camino, G.; Lomakin, S. M.; Lageard, M. Thermal Polydimethylsiloxane Degradation. Part 2. The Degradation Mechanisms. *Polymer* **2002**, *43*, 2011−2015.
(17) Deshpande, G.; Rezac, M. E. Kinetic Aspects of the Thermal Degradation of Poly(dimethyl siloxane) and Poly(dimethyl diphenyl siloxane). *Polym. Degrad. Stab.* **2002**, *76*, 17−24.
(18) Dvornic, P. R. Thermal Properties of Polysiloxanes. In *Silicon-Containing Polymers. The Science and Technology of their Synthesis and Applications*; Jones, R. G., Ando, W., Chojnowski, J., Eds.; Kluwer Academic Publishers: Dordrecht, The Netherlands, 2000; p 185.
(19) Mark, J. E. Silicon Containing Polymers. In *Silicon-Based Polymer Science; A Comprehensive Resource*; Ziegler, J. M., Fearon, F. W. G., Eds.; Advances in Chemistry Series, Vol. *224*; American Chemical Society: Washington, DC, 1990; p 47.
(20) Pauling, L. *The Nature of the Chemical Bond*, 3rd ed.; Cornell University Press: Ithaca, NY, 1960.
(21) Gillespie, R. J.; Johnson, S. A. Study of Bond Angles and Bond Lengths in Disiloxane and Related Molecules in Terms of the

Topology of the Electron Density and its Laplacian. *Inorg. Chem.* **1997**, *36*, 3031−3039.
(22) Hertel, T.; Jakob, J.; Minkwitz, R.; Oberhammer, H. Bonding Properties of Siloxanes: Gas Phase Structures of *N*,*N*-Bis-(trifluoromethyl)-*O*-(trimethylsilyl)hydroxylamine, $Me_3SiON(CF_3)_2$, and Trimethylsilyl Nitrate, Me_3SiONO_2. *Inorg. Chem.* **1998**, *37*, 5092−5096.
(23) Schwartz, M.; Berry, R. J. Ab Initio Investigation of Substituent Effects on Bond Dissociation Enthalpies in Siloxanes and Silanols. *J. Mol. Struct.: THEOCHEM* **2001**, *538*, 9−17.
(24) Almenningen, A.; Bastiansen, O.; Ewing, V.; Hedberg, K.; Trætteberg, M. The Molecular Structure of Disiloxane, $(SiH_3)_2O$. *Acta Chem. Scand.* **1963**, *17*, 2455−2460.
(25) Bakk, I.; Bóna, Á.; Nyulászi, L.; Szieberth, D. Modelling Extended Systems Containing Siloxane Building Blocks. *J. Mol. Struct.: THEOCHEM* **2006**, *770*, 111−118.
(26) This value was calculated in our laboratory.
(27) Smith, J. S.; Borodin, O.; Smith, G. D. A Quantum Chemistry Based Force Field for Poly(dimethylsiloxane). *J. Phys. Chem. B* **2004**, *108*, 20340−20350.
(28) The basis set superposition error computed with the counterpoise method is 1.9 kcal/mol at this level.
(29) Carteret, C.; Labrosse, A.; Assfeld, X. An Ab Initio and DFT Study of Structure and Vibrational Spectra of Disiloxane $H_3SiOSiH_3$ Conformers. Comparison to Experimental Data. *Spectrochim. Acta, Part A* **2007**, *67*, 1421−1429.
(30) Truhlar, D. G.; Isaacson, A. D. Simple Perturbation Theory Estimates of Equilibrium Constants from Force Fields. *J. Chem. Phys.* **1991**, *94*, 357−359.
(31) Truhlar, D. G.; Brown, F. B.; Steckler, R.; Isaacson, A. D. In *The Theory of Chemical Reaction Dynamics*; Clary, D. C., Ed.; D. Reidel Publishing Company: Dordrecht, The Netherlands, 1986; pp 285−329.
(32) Filho, H. P. M. Molecular Orbital Anharmonic Estimates for the Infrared Spectrum of CO_2. *Spectrochim. Acta, Part A* **2002**, *58*, 2621−2632.
(33) The anharmonicity correction was computed by going to second order in cubic force constants and first order in quartic force constants. The Coriolis interaction was also included in these calculations.
(34) Edinoff, M. L.; Aston, J. G. The Rotational Entropy of Nonrigid Polyatomic Molecules. *J. Chem. Phys.* **1935**, *3*, 379−383.
(35) Kilpatrick, J. E.; Pitzer, K. S. Energy Levels and Thermodynamic Functions for Molecules with Internal rotation. III. Compound Rotation. *J. Chem. Phys.* **1949**, *17*, 1064−1075.
(36) The expressions given in ref 35 are specific for internal rotors that are off-balanced in one direction only. The most general procedure was used in our work. See the Appendix in: Kharroubi, M.; de Sainte Claire, P. The Pitzer Free Rotor for Nondegenerate Modes: Application to the Long-Range Behavior of Halogen Radical Reactions with Substituted Olefins. *J. Phys. Chem. A* **2003**, *107*, 4483−4489.
(37) Van Speybroeck, V.; Vansteenkiste, P.; Van Neck, D.; Waroquier, M. Why does the Uncoupled Hindered Rotor Model work well for the Thermodynamics of *n*-alkanes? *Chem. Phys. Lett.* **2005**, *402*, 479−484.
(38) Vansteenkiste, P.; Van Speybroeck, V.; Pauwels, E.; Waroquier, M. How should we Calculate Multi-dimensional Potential Energy Surfaces for an Accurate Reproduction of Partition Functions? *Chem. Phys.* **2005**, *314*, 109−117.
(39) Our computer program was able to reproduce the 1D-HR results given in refs 37 and 38. These calculations were performed for the sake of comparison.
(40) This variation was fit with a series of cosine functions: $f(\varphi_i) = p_0 + (1/2)\sum_{k=1}^{3} p_k[1 - \cos k(\varphi_i - p'_k)]$. D in eq 3 is maximum at the equilibrium geometry ($D_{max} = D_0$).
(41) Benson, S. W. *Thermochemical Kinetics*, 2nd ed.; Wiley: New York, 1976.
(42) Frisch, M. J.; Trucks, G. W.; Schlegel, H. B.; Scuseria, G. E.; Robb, M. A.; Cheeseman, J. R.; Montgomery, J. A., Jr.; Vreven, T.; Kudin, K. N.; Burant, J. C.; et al. *Gaussian 03*, revision B.05; Gaussian, Inc.: Wallingford, CT, 2004.
(43) de Sainte Claire, P., Song. K.; Hase, W. L.; Brenner, D. W. Comparison of Ab Initio and Empirical Potentials for H-Atom Association with Diamond Surfaces. *J. Phys. Chem.* **1996**, *100*, 1761−1766 (footnote in Table 3).
(44) PV is included in 4*RT*.
(45) The hindered rotor contribution is the same for L_n and $L_{n-x} + D_x$ as long as x is large (the number of chain-like hindered rotors is $2n$ overall on each side of the equilibrium). The vibrational contribution difference between L_n and $L_{n-x} + D_x$ becomes constant for large cycles (see text). In eq 7, $S^{D_8}_{vib}$ does not include hindered rotor contributions because all the degrees of freedom of the small cycles ($x \leq 5$) were treated as pure vibrations.
(46) It does not mean that half of the entropy is configurational. Consider a hypothetic species D'_8 where entropy $S_{D'_8}$ is purely configurational, i.e., a species that is described by the RIS model. In our calculation, $0.5 \times S_{D'_8}$ (50% of $S_{D'_8}$) amounts to a fraction of the total entropy of D_8. However, in this case, the hindered rotor entropy is significant and much larger than $0.5 \times S_{D'_8}$. Thus, p_3 smaller than p_1 means that the contribution of configurational entropy has a smoothing effect on $\log(K_x) = f(x)$. Accordingly, 50% of $S_{D'_x}$ represents a larger contribution of the total entropy when x becomes larger, because the hindered rotor contribution in that case becomes smaller.
(47) For T = 383.15 K, c_3 = 23.79 cal/mol/K, c_4 = 6.052 cal/mol/K, c_5 = 0.659, and c_6 = 0.7.
(48) The largest difference was observed for D_4, where $\log(K_4)$ = −0.48 at 383.15 K, while it was −0.69 at 273.15 K.